

Biphasic Nature of Lipid Bilayers Assembled on Silica Nanoparticles and Evidence for an Interdigitated Phase

*Dillan Stengel, Rich Thai, Yuan Li, Nikki M. Peters, Gregory P. Holland**

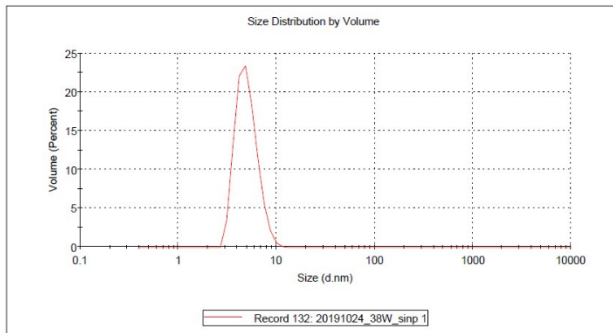
Department of Chemistry and Biochemistry, San Diego State University, 5500 Campanile Dr.
San Diego CA, 92182-1030 USA

*Corresponding Author Email: gholland@sdsu.edu

A

	Size (d.nm):	% Volume:	St Dev (d.nm):
Z-Average (d.nm): 32.84	Peak 1: 4.072	99.9	1.290
Pdl: 0.021	Peak 2: 92.19	0.1	83.69
Intercept: 0.754	Peak 3: 0.000	0.0	0.000

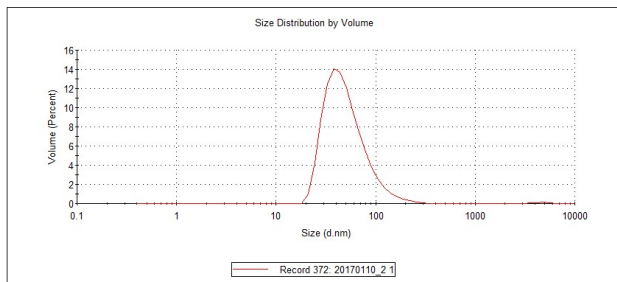
Result quality : **Good**



B

	Size (d.nm):	% Volume:	St Dev (d.nm):
Z-Average (d.nm): 75.93	Peak 1: 53.37	99.6	29.84
Pdl: 0.206	Peak 2: 4802	0.4	870.5
Intercept: 0.937	Peak 3: 0.000	0.0	0.000

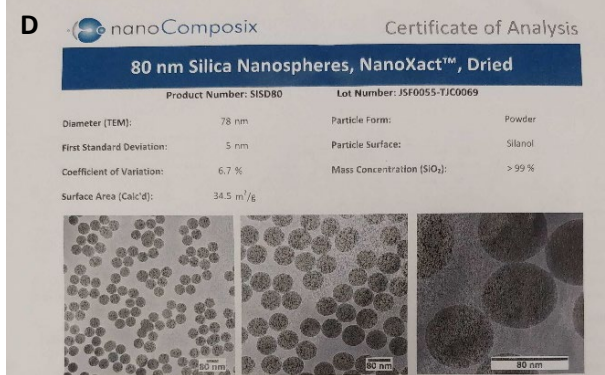
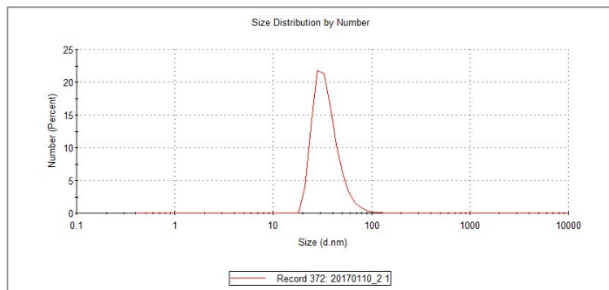
Result quality : **Good**



C

	Size (d.nm):	% Number:	St Dev (d.nm):
Z-Average (d.nm): 75.93	Peak 1: 35.30	100.0	11.77
Pdl: 0.206	Peak 2: 0.000	0.0	0.000
Intercept: 0.937	Peak 3: 0.000	0.0	0.000

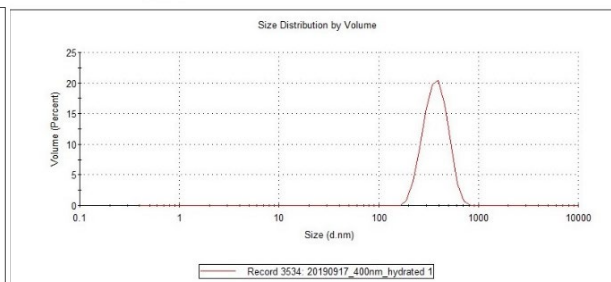
Result quality : **Good**



E

	Size (d.nm):	% Volume:	St Dev (d.nm):
Z-Average (d.nm): 337.9	Peak 1: 381.3	100.0	101.1
Pdl: 0.060	Peak 2: 0.000	0.0	0.000
Intercept: 0.918	Peak 3: 0.000	0.0	0.000

Result quality : **Good**



F

	Size (d.nm):	% Volume:	St Dev (d.nm):
Z-Average (d.nm): 129.4	Peak 1: 127.5	100.0	41.16
Pdl: 0.063	Peak 2: 0.000	0.0	0.000
Intercept: 0.944	Peak 3: 0.000	0.0	0.000

Result quality : **Good**

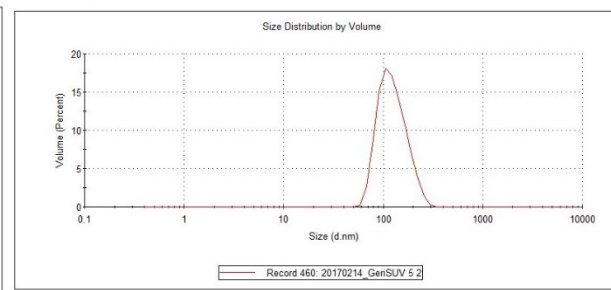


Figure S1. DLS of Stöber-synthesized nanoparticles and DMPC SUVs after extrusion. The nominal diameters for each are: A, 4 nm; B, 53 nm (by volume); C, 35 nm (by number); D, 80 nm; E, 400 nm; F, 128 nm for SUVs extruded with a 100 nm filter. The graphs in B and C are from the same sample, but are reported using either the volume distribution (B) or number distribution (C). The number distribution more accurately reflects the total surface area of this sample which is reported in Supplementary Table 1. Figure S2B shows TEM images of this sample. The certificate of analysis for the nominal 80 nm particles (D) are from the manufacturer.

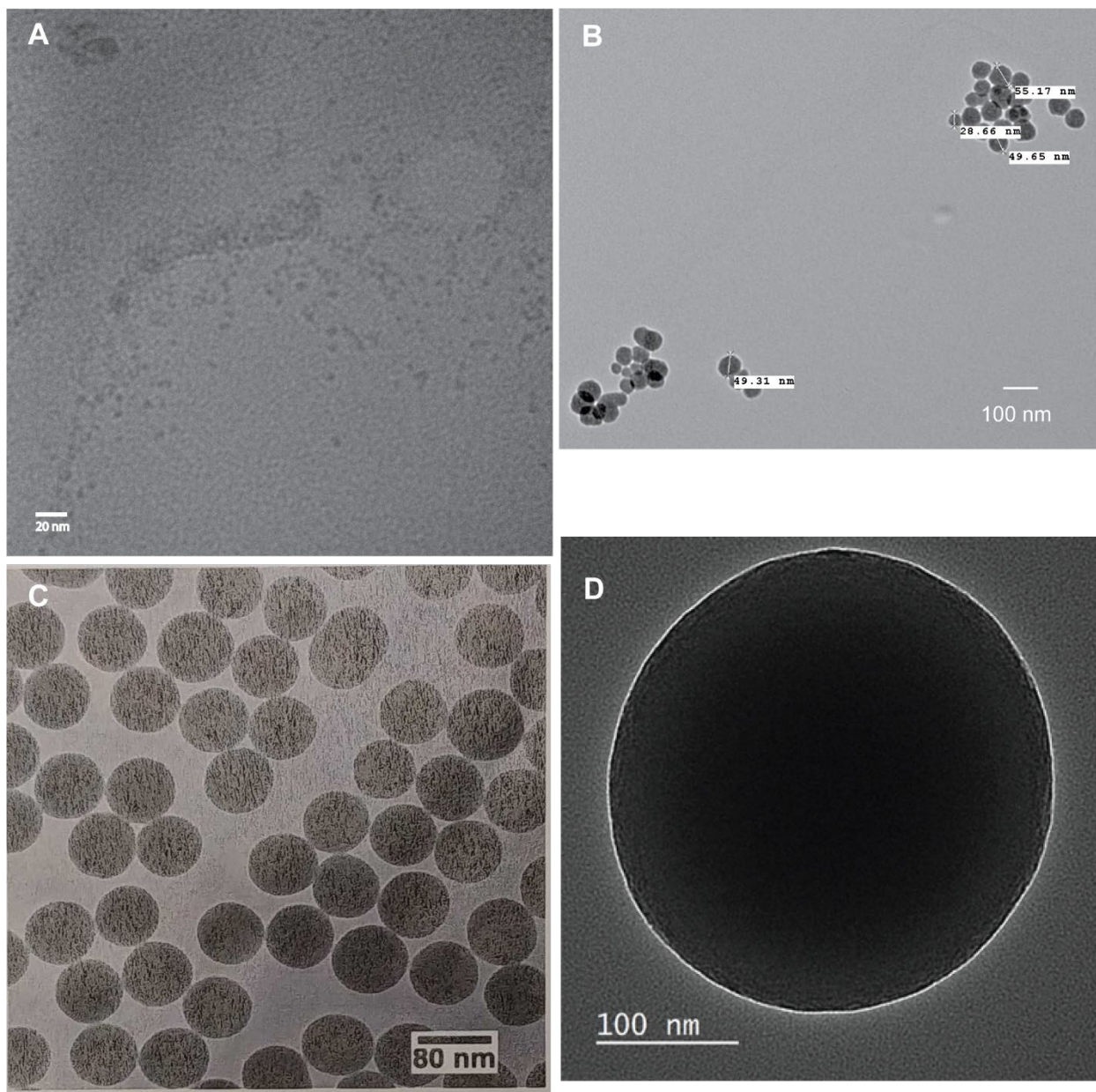


Figure S2. TEM images of uncoated silica nanoparticles. A, 4 nm. B, 35 nm. C, 78 nm, and D, 381 nm. Sizes reported here are from DLS data in Figure S1. Samples were imaged using an FEC Tecnai 12 TEM.

Table S1. Calculated lipid weight loss on various SSVs from TGA. Nanoparticle sizes are listed as \pm SD that is based on DLS or a certificate of analysis (Figure S1). Bare nanoparticles were soaked in water before TGA analysis to calculate the loss of water adsorbed to the uncoated nanoparticles. Calculated weight loss is the difference between the coated nanoparticles and the soaked bare nanoparticles (representative TGA data shown in Figure S3). Theoretical weight loss is assuming a planar surface of a single bilayer of lipids on the nanoparticle. Because of the large distribution in the 53 nm sample (\pm 30 nm, Supplementary Figure 2) we have also included the size by number density (35 nm), which is in better agreement with the theoretical weight loss and TEM (Figure S2).

Diameter (nm)	Coated Start (mg)	Coated End (mg)	% wt Loss	Bare Start (mg)	Bare Finish (mg)	% wt Loss	Calculated Weight Loss (%)	Theoretical Weight Loss (%)
381 \pm 101	49.42	44.77	9.4	14.86	13.85	6.8	2.61	2.46
78 \pm 5	47.31	40.42	14.6	11.5	11.1	3.5	11.10	10.31
53 \pm 30	43.94	33.51	23.7	30.18	29.66	1.7	22.03	15.25
35 \pm 12 †								21.42
4 \pm 1	25.01	5.97	76.1	5.55	5.37	3.2	72.9	70.50

† size by number

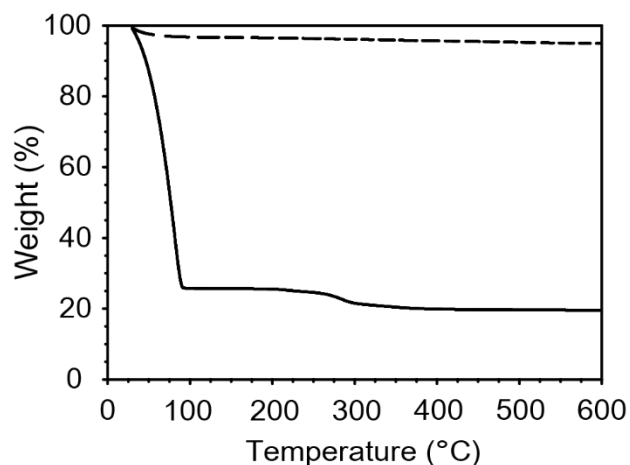


Figure S3. Example TGA trace of bare nanoparticles in water (dashed line) and DMPC-coated 78 nm silica nanoparticles (solid line). Weight loss of the coated nanoparticles was calculated from the weight at 50°C minus the weight at 600°C.

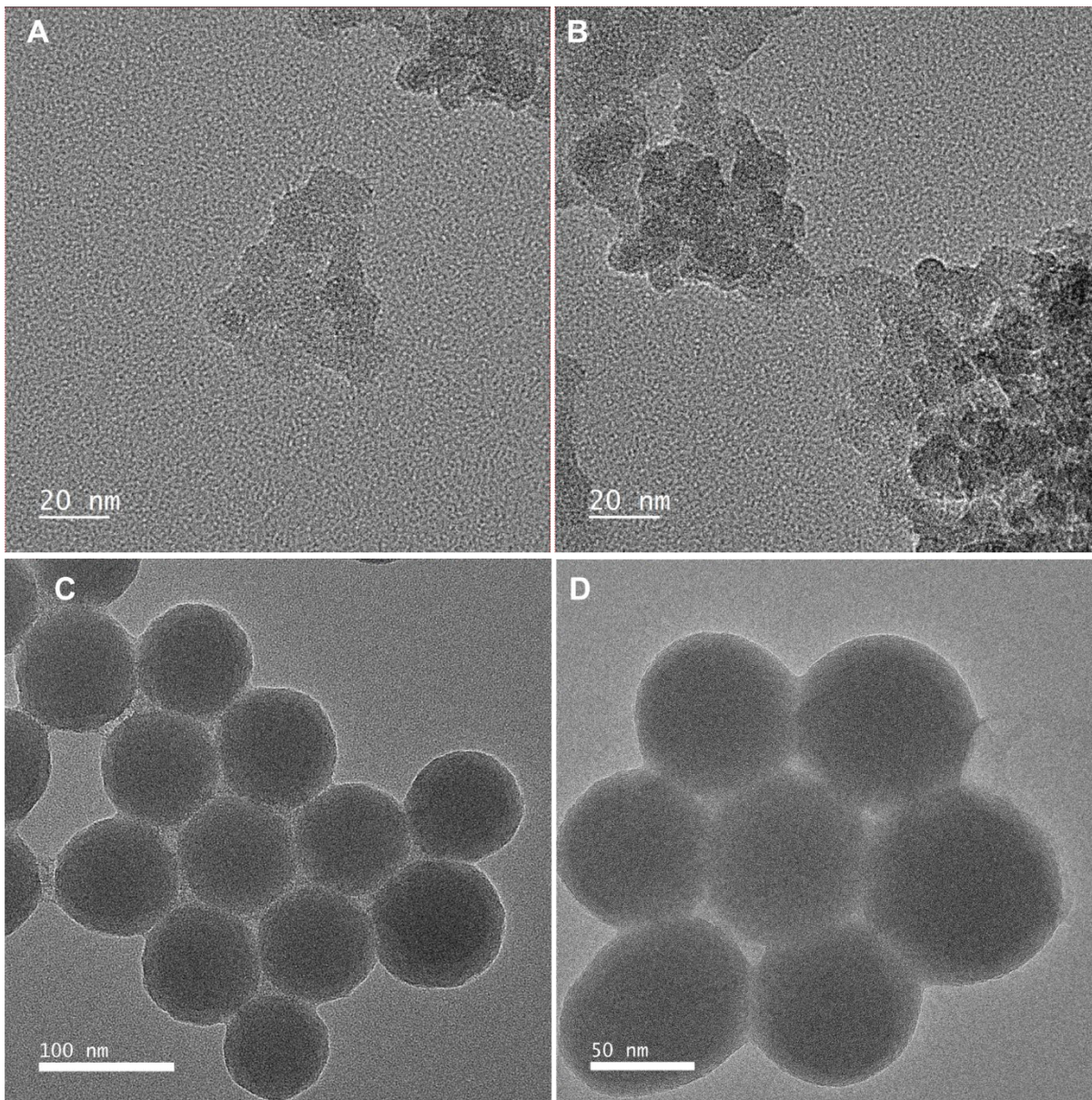
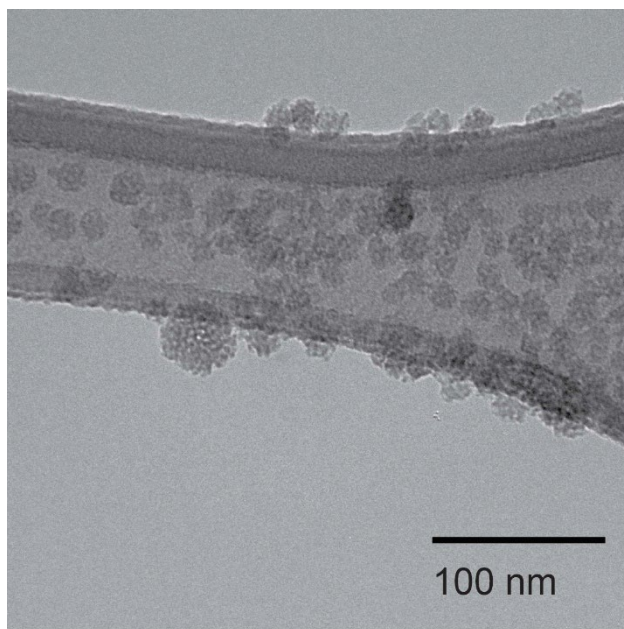


Figure S4. TEM images of DMPC-coated silica nanoparticles. A and B, 4 nm. C and D, 78 nm. Sizes reported here are from DLS data shown in Figure S1. Samples were imaged using a FEI Tecnai 12 TEM.



Diameter (nm)	Coated Start (mg)	Coated End (mg)	% wt Loss	Bare Start (mg)	Bare Finish (mg)	% wt Loss	Calculated Weight Loss (%)	Theoretical Weight Loss (%)
20 nm	4.785	3.889	18.725	6.579	6.371	3.165	15.56	67.57 (using surface area 545.9 m ² /g)

Figure S5. TEM image of 20 nm MSN nanoparticles with 2 nm pores (top) and TGA data for lipid coated MSN SSVs. The calculated weight loss from TGA roughly agrees with that expected for a nonporous, colloidal silica sphere (Table S1) indicating that the lipid bilayer is not incorporated in the pore space and only exists on the surface of the particle analogous to the colloidal SSVs.

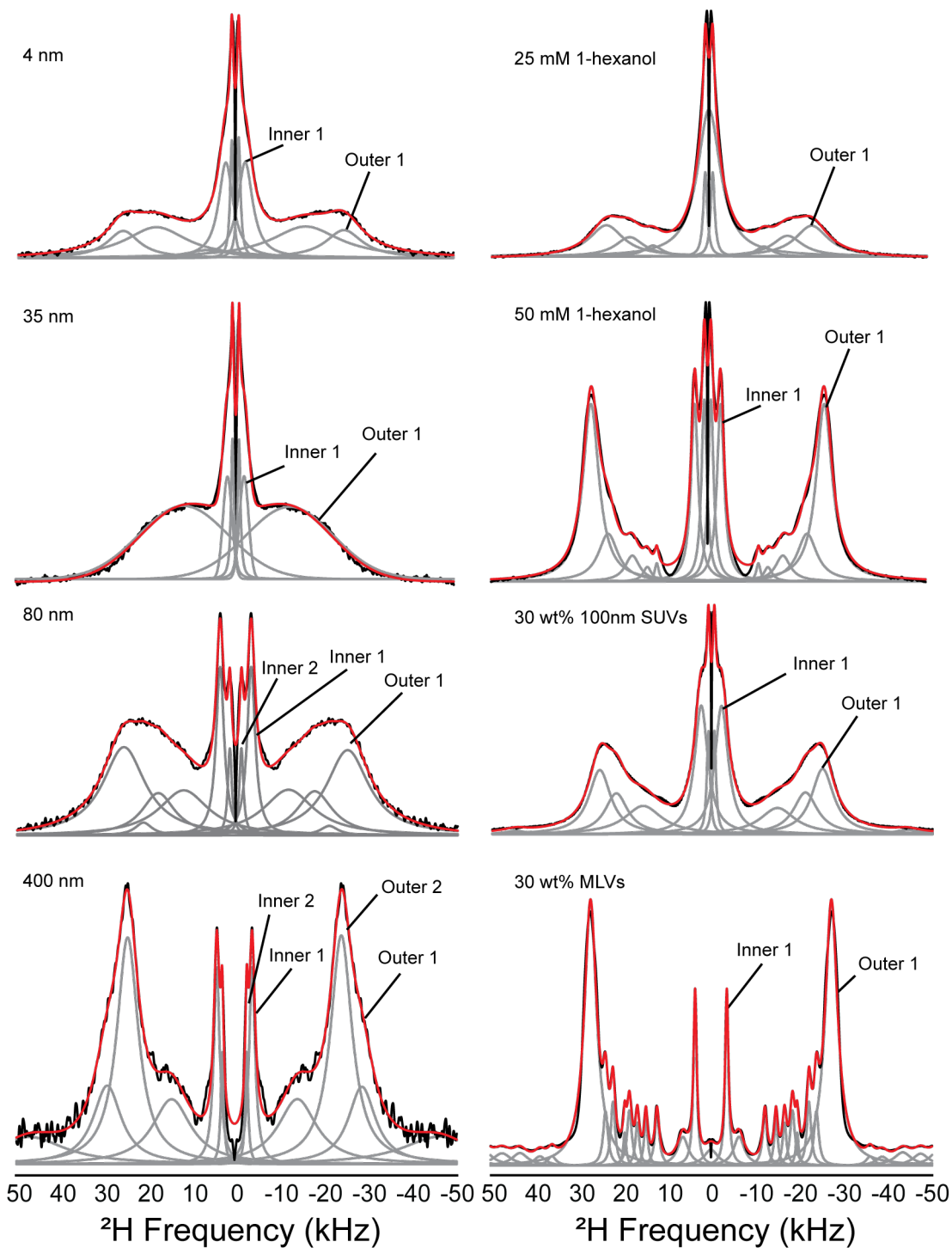


Figure S6. Deconvolutions of de-Paked ^2H solid-state NMR spectra for SSVs and lipid bilayer controls. The splitting for the inner-most and outermost peaks correspond to the terminal methyl CD_3 and CD_2 groups nearest the head group, respectively. The ^2H splittings for SSVs are reported in the main text, Table 1. DMFIT was used to deconvolute the spectra.

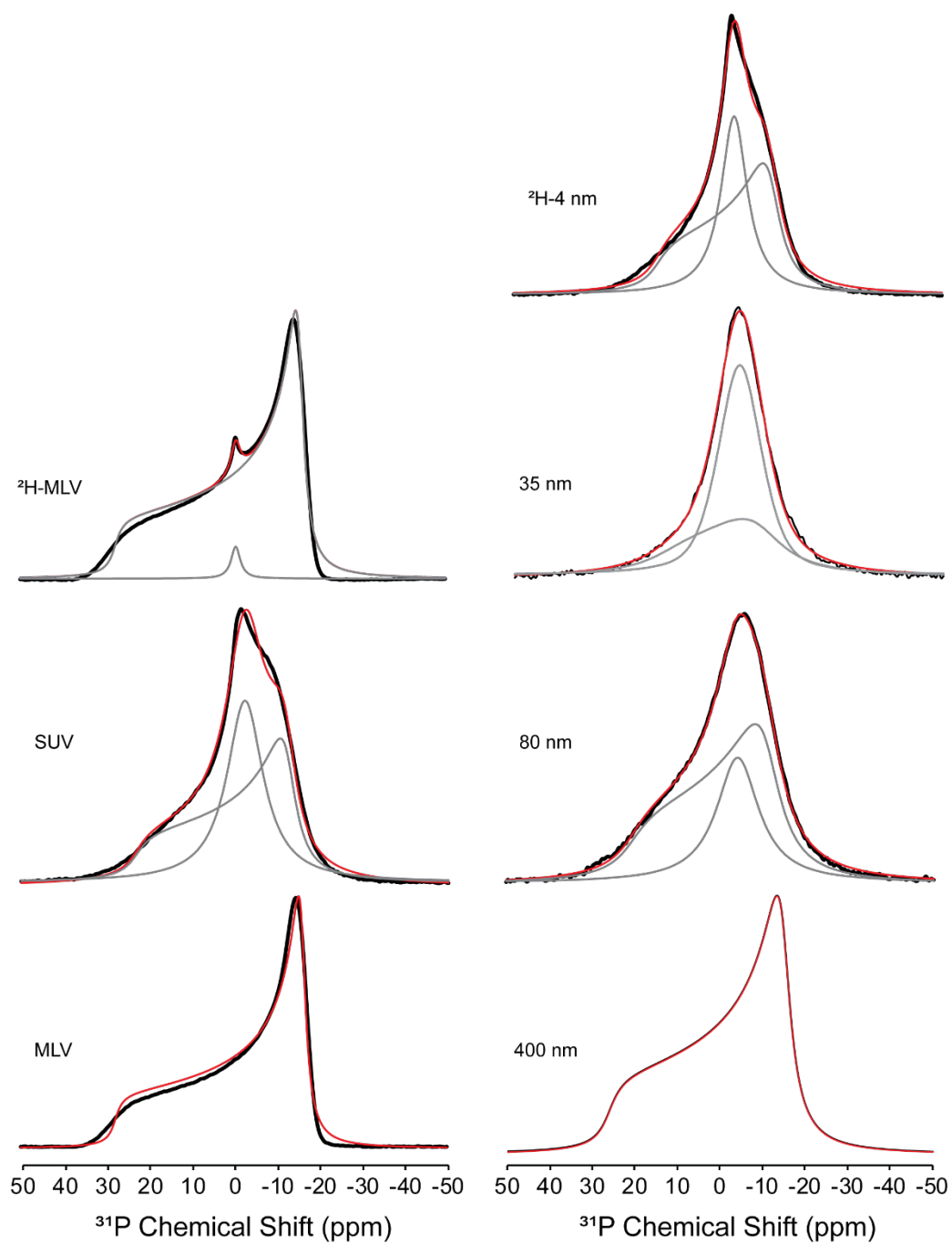


Figure S7. ^{31}P CSA fits for SSVs. Deconvoluted isotropic and CSA fits are in grey and their sum shown in red. The original spectra are black. The ^{31}P CSA and ratio of anisotropic to isotropic components extracted from the fits is presented in Table 2 of the main text along with CSA parameters. The asymmetry parameter (η) was 0 for all CSA fits consistent with the L_{α} lamellar bilayer phase.

Table S2. ^{31}P NMR T_1 and T_2 relaxation times of DMPC lipid samples. The SUV and MLV samples are 30 wt%.

°C	T_1 (ms)						
	4 nm*	35 nm	80 nm	400 nm	100 nm SUV	400 nm SUV	MLV
50							735
40						132	656
35	601	309	656	533	643	139	635
30	597	323	654	563	650	164	639
25	635	352	710	551	682	192	647
20	752	481	897	896	804	253	782
15	866	580	1019	894	806	295	902
10	974	616	1153	884	972	342	906
5	1074						
T_2 (μs)							
50							923
40						206	1004
35	513	400	470	1057	718	247	1407
30	535	382	495	1224	810	281	1596
25	555	346	569	1263	1031	359	2826
20	587	313	672	965	1018	621	939
15	867	240	730	889	1030	693	1009
10	951	253	784	873	912	663	951
5	853						

* coated with DMPC- d_{54}

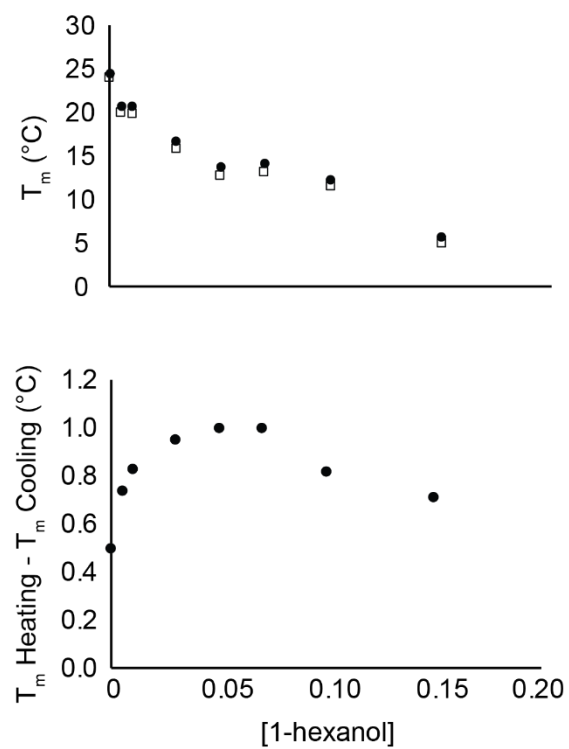


Figure S8. Recorded DSC T_m of SUVs (top) during heating (circles) and cooling (squares) cycles and their differences (bottom) as a function of 1-hexanol concentration. The greatest difference is observed at 50 mM 1-hexanol and indicates the largest degree of interdigitation occurs at this concentration.

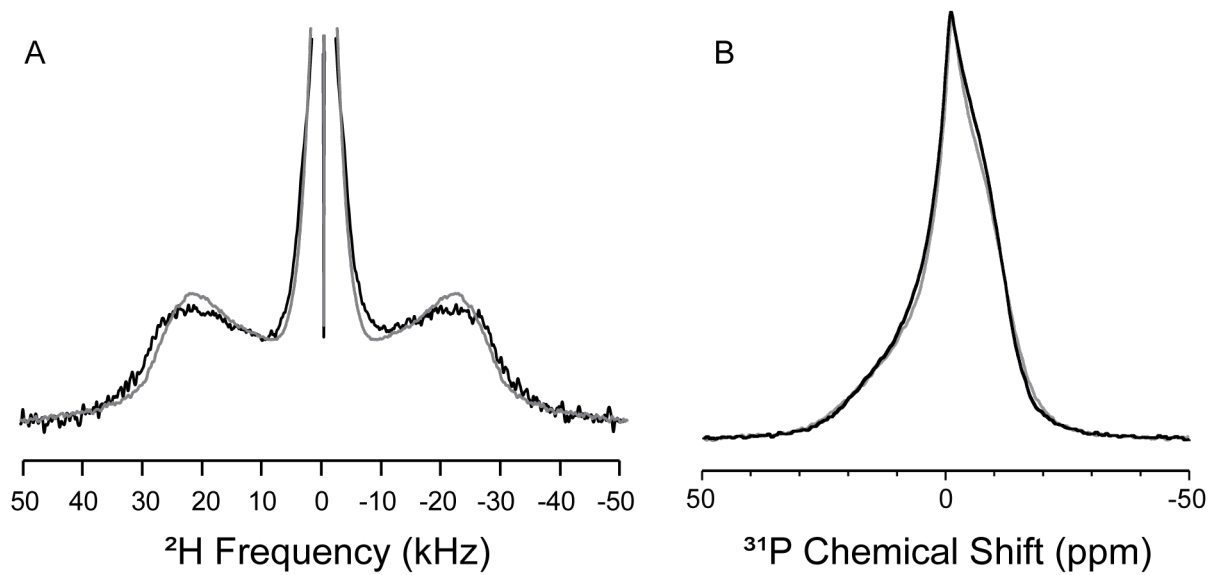


Figure S9. De-Paked ^2H (A) and ^{31}P (B) solid-state NMR spectra of 4 nm SSVs (black) and 100nm SUVs interdigitated with 25 mM 1-hexanol at 20 wt% (grey) and 30°C.

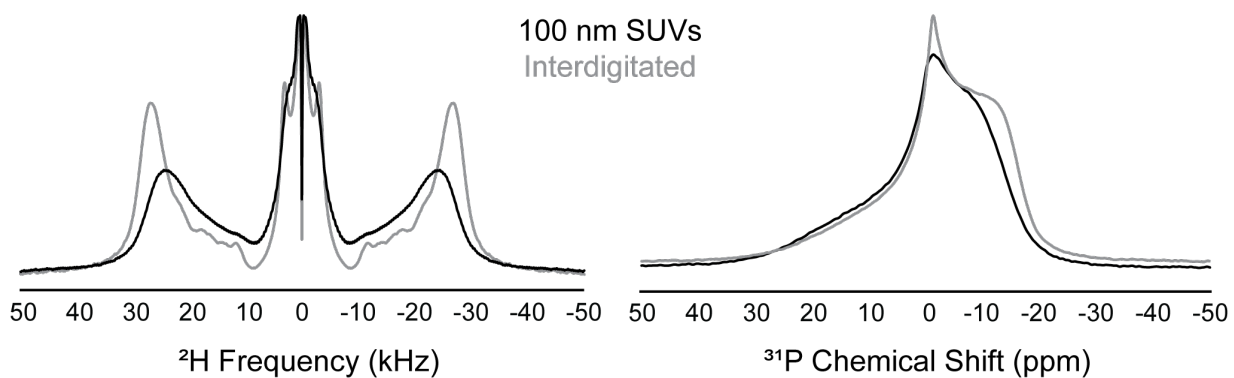


Figure S10. Static solid-state ^2H and ^{31}P NMR spectra of 20 wt% DMPC- d_{54} SUVs (black) and the same sample interdigitated with 50 mM 1-hexanol (grey) at 30 °C. In the ^2H spectra, the splitting for the outer peaks is wider for the interdigitated spectra compared to the SUV and the ^{31}P spectrum displays a slightly larger CSA for the interdigitated phase.

